SPRAYED BORIC ACID AS A DOPANT SOURCE FOR SILICON RIBBONS

J. A. Silva, M. C. Brito, I. Costa, J. Maia Alves, J. M. Serra and A. M. Vallêra
CFMC / Departamento de Física da Faculdade de Ciências da Universidade de Lisboa
Campo Grande Edifício C8, 1749-016 Lisboa, Portugal

ABSTRACT: This paper presents a new method for bulk boron doping of silicon ribbons for solar cells. The method is based on the spraying of the ribbon with a solution of boric acid followed by zone melting recrystallization in an argon atmosphere. Dopant incorporation is evaluated by measuring the spreading resistance of the silicon ribbon.

A numerical model for the incorporation of boron into silicon was developed, considering two competing mechanisms: boron diffusion during the heating step and evaporated boron transport in the gas phase. The dependence of the incorporation of boron on experimental parameters such as the direction of recrystallization and the flux of argon in and out of the furnace was measured, yielding results that are compatible with the numerical model. It is also shown that the mean incorporation of boron into the samples depends linearly on the initial concentration of boric acid.

Keywords: Doping, Ribbon Silicon, Zone melting.

1 INTRODUCTION

Crystalline silicon wafers produced from ingots, either multicrystalline or monocrystalline grown using the Czochralski method, are usually doped by adding to the feedstock material heavily boron doped silicon pellets. On the other hand, silicon material grown from silane or chlorosilanes, such as that in amorphous or microcrystalline silicon films, is doped using an atmosphere which includes the dopant, for instance in the form of diborane gas. These techniques, however, are less suited for methods of crystalline sheet silicon growth such as those based on zone melting recrystallization (ZMR), when the pre-ribbon is best produced undoped [1–4]. In this paper we report on a new method for bulk doping crystalline silicon ribbons using sprayed boric acid as the dopant source. The method is compatible with an in-line transport system, is reliable and easily controllable, and uses an inexpensive and widely available dopant source.

The method is based on the spraying of intrinsic silicon pre-ribbons with a solution containing boric acid. This pre-ribbon is then subjected to zone melting recrystallization in an argon atmosphere. As the temperature increases, the boric acid decomposes into boron oxide and water [5], the latter being evaporated from the surface of the sample. For temperatures above 1300K, boron is incorporated into the sample by diffusion across the surface [6] forming silicon oxide according to the reaction described by equation (1)

$$2B_2O_3(g) + 3Si(s) \rightarrow 3SiO_2(s) + 4B(s) \qquad (1)$$

However, when the sample reaches 1400K, most of the boric oxide has evaporated from the surface of the sample therefore removing the boron source for the diffusion process [7]. The argon-boron atmosphere will then be responsible for further doping of the silicon with boron. In the molten zone the boron will be uniformly mixed due to convection in the liquid.

The measurement of the incorporation of boron into the silicon samples was undertaken by measuring the sheet resistance of the samples, using the four point probe method. It was assumed that all boron atoms incorporated in the sample are electrically active.

This paper describes a simple numerical model of the boron incorporation into the silicon and experimental results that demonstrate the feasibility of this doping method. It is shown that one may control the incorporation of boron by changing the initial concentration of boric acid on the surface of the sample. It is also established how the incorporation of boron depends on parameters such as the direction of recrystallization and the flux of argon in and out of the furnace.

2 BORON INCORPORATION MECHANISMS

Let us start by considering a silicon sample sprayed with a solution of boric acid (H_3BO_3) in water. During the zone melting recrystallization process an elemental cell of the sample will suffer a heating process with the arrival of the molten zone (see fig. 1).

As the temperature of the cell increases above 170ºC, the water molecules in the solution will have been vaporized and boric acid becomes metaboric acid (HBO_2) via the reaction described by equation (2.1), further releasing water molecules. As the temperature is increased, metaboric acid becomes boron oxide (B_2O_3) via the reaction described by equation (2.2). Boric acid may also free water molecules and become boron oxide, via the reaction described by equation (2.3), without passing the metaboric acid phase.

$$H_3BO_3 \rightarrow HBO_2 + H_2O \quad (2.1)$$

$$2\,HBO_2 \rightarrow B_2O_3 + H_2O \quad (2.2)$$

$$2\,H_3BO_3 \rightarrow B_2O_3 + 3\,H_2O \quad (2.3)$$

The solubility diagram of the H_3BO_3-B_2O_3 system [5] shows that for temperatures above 450ºC all boron atoms will be present as boron oxide. Since this is also the fusion temperature of boron oxide, at this temperature all the sprayed boron atoms will be on the surface of the sample in the form of liquid boron oxide. By a further increase in temperature, the boron oxide will be evaporated, without any significant dissociation [8].

The boron oxide evaporation rate per unit area, m, at temperature T, may be described [9] by equation (3)

$$m(T) = p_v \sqrt{\frac{M}{2p\,RT}} \quad (3)$$

where M is the molecular mass of B_2O_3 and p_v its vapour pressure, which is given by van Hoff's equation [10]

$$p_v = p_0 \exp\left(-\frac{\Delta H_{vap}(T)}{RT} + \frac{\Delta S_{vap}(T)}{T} \right) \quad (4)$$

where p_0 is the pressure of the system and DH_{vap} and DS_{vap} are the change in enthalpy and entropy at the gas-liquid phase transition, respectively. These thermodynamic coefficients were obtained for the relevant range of temperatures (900–1500ºC) using empirical data [7].

The evaporation rate determines the mass evaporation of the boron oxide through equation

$$\frac{dm}{dt} = -Am \qquad (5)$$

where m is the mass of boron oxide still on the surface of the sample and A is its effective surface area. Assuming that the boron oxide is deposited as small thin film disks uniformly distributed on the ribbon surface one may assume that A/m is constant and therefore equation 6 yields

$$\frac{m}{m_0} = \frac{A}{A_0} = 1 - e^{-\frac{A_0}{m_0}\int_0^t m\,dt} \qquad (6)$$

This solution underestimates the boron oxide evaporation time because it does not consider the thinning of the boron oxide layer with evaporation. If a semi-spherical shape for the boron oxide drop was assumed, its height would decrease proportionally with its radius and the evaporation time would be about two orders of magnitude larger. In order to account for this effect we have introduced a form factor parameter a = 30, which is closer to the thin boron oxide film approach, a choice confirmed by the experimental measurement of the height of the boron oxide drop (see experimental section below).

In the example shown in fig. 2 we have considered a temperature gradient of 50K/mm which is the typical temperature gradient for our experimental conditions [11]. This plot shows that when the temperature reaches 1500K (about 2 minutes, for typical operating velocities) the boron oxide has evaporated from the surface of the sample.

Since most boron oxide evaporates into the atmosphere well before reaching the fusion temperature for silicon (1687K) [12] one concludes that only two types of incorporation of boron atoms in the silicon ribbon are important: boron diffusion from the surface into the solid silicon sample (before boron evaporation completes), and incorporation from the atmosphere into the melt.

Assuming that the amount of boron oxide on the surface is determined by the evaporation process and not by the diffusion process, the latter may be described by the solution of Fick's equation for a constant dopant source [6] and therefore the concentration C at time t and depth x is given by

$$C(x,t) = C_s erfc\left(\frac{x}{2\sqrt{Dt}}\right) \qquad (7)$$

where C_s is the surface concentration of boron atoms (or the solubility limit of boron in silicon) and D the diffusion coefficient of boron in silicon. Integrating over the thickness s of the sample we get

$$C(t) = \int_0^s C_s erfc\left(\frac{x}{2\sqrt{Dt}}\right)dx = \frac{2}{\sqrt{p}} C_s \sqrt{Dt} \qquad (8)$$

Using available data for the temperature variation of the solubility limit [12] and the diffusion coefficient [6] we can calculate the boron incorporation rate in the sample during the heating process (fig. 3). The diffusion process described by equation (7) has been coupled with the evaporation equation (4).

We can see that as the temperature increases the boron incorporation increases due to the increase of the diffusion coefficient with temperature. Above 1375 K the incorporation rate decreases due to the fact that less boron oxide is available on the surface. Integrating these results over time we determine the final incorporation of boron atoms in the silicon sample. For these particular experimental conditions (see details below in the experimental section) an incorporation of 8.1% is predicted (fig. 4).

When the temperature of the sample reaches 1687K, the melting temperature of silicon, the boron atoms available in the atmosphere will determine any further incorporation. The efficiency of this second incorporation mechanism will depend critically on the experimental operating conditions. On one hand, part of the evaporated boron oxide will be dragged outside by the cleaning argon circulation. On the other hand, if the molten zone is moving upwards (i.e. the sample is moving downwards between the stationary halogen lamps, as shown in fig. 1) the evaporated boron oxide molecules, dragged by upward convection currents, will either be incorporated into the sample by sticking to the molten zone, or deposited further up on the surface of the sample and repeat the evaporation/diffusion process described earlier. If, however, the molten zone is moving downwards (i.e. the sample is moving upwards) the boron oxide molecules transported by the convection currents will preferably be deposited in a region of the sample which is already cooling and therefore will have little chance of being incorporated into the sample.

3 EXPERIMENTAL PROCEDURE

3.1 Samples

Since the goal of this work was solely to demonstrate the feasibility of the doping process, the samples used were already doped, with initial carrier concentrations of the order of 10^{16} cm^{-3} and ended with uniform doping levels in the range 10^{17}–10^{18} cm^{-3} after recrystallization. The pre-ribbons were 100×30×0.3 mm^3 multicrystalline silicon wafers from Deutsche Solar.

3.2 Boric acid deposition

The doping process begins with sample cleaning with POLISH ($HF+HNO_3+CH_3COOH$) and HF solutions. Then, the samples are sprayed with a solution of boric acid with a concentration of 0.1365 mol/l.

The spraying of the boric acid is carried out using an airbrush Badger 250 fed with a fixed pressure of nitrogen in order to guarantee a reproducible and homogeneous deposition. The airbrush is located 80 cm above the sample. A 22 cm diameter cylindrical enclosure is used to prevent perturbations due to air currents.

Figure 5 shows a microscopy photograph of the deposited boric acid after drying. The boric acid aggregates are more or less planar circles with typical 100μm diameter and an average height 3.3μm. Statistical analysis of such microscopy images allows us to estimate the deposited area to be of the order of 1% of the total sample area. The estimation of the area of deposited boron oxide (at 450ºC) may be made assuming that the variation of the area of the deposit is proportional to the variation of the deposit mass due to reactions (2.1) to (2.3).

3.3 Recrystallization

The molten zone is created by focusing radiation from two 1000 W halogen light bulbs onto a narrow line, 2mm wide, as shown in fig. 1. In a typical run, the sample is moved downwards with a 3mm/min velocity and the atmosphere inside the furnace is renewed with a 1.1 l/min argon flux.

After recrystallization, the sample is cleaned with an HF solution that removes the layer of silicon oxide from the surface.

3.4 Concentration of carriers

The concentration of charge carriers, N, is calculated from the sample resistivity, r, using the relationship

$$r = \frac{1}{qN m_p} \qquad (9)$$

where q is the charge of the electron and m_p is the hole mobility. The hole mobility was determined from data for doping dependent hole mobility in silicon at 300 K [12]. Resistivity was determined by multiplying the sheet resistance, measured using a standard four point probe system, by the sample thickness, measured with a differential mechanical profilometer developed on our laboratory [13].

4 RESULTS

4.1 Boron incorporation rate

It was observed that the mean incorporation of boron into the samples depends linearly on the initial concentration of boric acid. This result is shown in Fig. 6, where the boron concentration in the recrystallized sample, N, is plotted as a function of the initial concentration of boric acid, N_{dep}, for typical run parameters (sample moving downwards at 3mm/min, argon flux 1.1 l/min).

Sheet resistance measurements on both surfaces of the samples also show that the convection in the melting zone is sufficient to redistribute the incorporated boron homogeneously across the sample thickness.

4.2 Effect of recrystallization direction

As discussed above, the incorporation of boron into the sample is achieved through two different mechanisms, solid state diffusion and vapor-phase incorporation, the latter having a fundamental incorporation efficiency asymmetry depending on the direction of recrystallization. In order to test this hypothesis, a series of experiments were performed spraying the sample surface across a mask, depositing the boric acid solution in only half of the sample. On the non-sprayed half of the sample surface the only source of boron incorporation will be the vapor-phase mechanism.

The results, shown in fig. 7, show that when the molten zone is moving upwards there is an extension of boron incorporation beyond the initial spraying step with an characteristic length of 7mm, which is much larger than what could be attributed to 4mm long combined effect of the spreading area of measurement of the sheet resistance and the width of the molten zone. If, however, the molten zone is moving downwards, this extension is only of about 5mm thus confirming that the vapor phase incorporation is indeed more efficient in the first case than in the second.

Running a series of experiments spraying the whole sample, we observed that the overall boron incorporation rate is higher when the molten zone is moving upwards (17.3±0.7%) than when recrystallization is performed in the opposite direction (11.9±0.1%) (see Fig. 8). These results again support the boron incorporation mechanisms described above.

Fig. 8 also shows the mean boron incorporation for multipass molten zone recrystallization experiments. As expected, the highest incorporation rate is achieved for the configuration where in the

first pass the molten zone is moving upwards (18.7 ± 1.8%) and the least favorable configuration is single pass with the molten zone moving downwards. From these results we conclude that, for these experimental conditions, the incorporation of boron due to the solid state diffusion is of the order of 10% of the initial deposited concentration whilst the remaining boron is incorporated from the vapor phase, directly into the molten silicon.

4.3 Effect of argon flux

The flux of argon in the furnace will also have an impact on the boron incorporation rate (Fig. 9).

One can see that the doubling of the argon flux (from 1.1 l/min to 2.2 l/min) significantly reduces the rate of incorporation of boron. This effect may be attributed to the fact that a larger argon flux drags a higher proportion of boron oxide from the atmosphere to the outside, thus reducing the incorporation of evaporated boron.

5. CONCLUSIONS

We have demonstrated a new process for bulk doping of crystalline silicon wafers using sprayed boric acid followed by zone melting recrystallization. During the heating process, as the molten zone approaches, the boric acid turns into boron oxide which diffuses into the solid silicon sample; the diffusion is halted when the dopant source is depleted through evaporation. Depending on the experimental conditions, evaporated boron oxide may be deposited further up the sample and repeat the evaporation/diffusion process. These incorporation mechanisms have been modelled numerically.

Experimentally, the method proved to efficiently modify the concentration of charge carriers in the sample as its variation depends linearly on the amount of boric acid deposited. The effects of the argon flux, the number of passes, and the direction of recrystallization on the boron incorporation were also studied and the experimental results validate the numerical model.

Sheet resistance measurements on both surfaces of the sample show that the convection in the liquid silicon upon melting is sufficient to redistribute the incorporated boron homogeneously across the thickness of the sample.

6 ACKNOWLEDGEMENTS

This work has been partially supported by FCT grants SFRH/BD/12763/2003 and SFRH/BPD/20660/2004.

7 REFERENCES

[1] R.M. Gamboa et al, Proc. 16th European PV Solar Energy Conference Glasgow (2000) 1598-1601.
[2] R.M. Gamboa et al, Solar Energy Materials & Solar Cells 72 (2002) 173-181.
[3] C.R. Pinto et al, Solar Energy Materials & Solar Cells 72 (2002) 209-217.
[4] C.R. Pinto et al, Proc. 21st European PV Solar Energy Conference Dresden (2006) 1099-1100
[5] F. C. Kracek et al, American Journal of Science 35A (1938) 142-171.
[6] J.C.C. Tsai “VLSI Technology”, S. M. Sze chapter 7(McGraw-Hill International Editions, 1998).
[7] Chase et al, Thermochemical Tables Journal of Physical Chemistry 14, Suppl 1 (1985).

[8] R. Speiser, S. Naiditch and H. L. Johnston, J. Am. Chem. Soc. 72 (1950) 2578-2580.

[9] I. Langmuir, Physical Review, 2nd Series vol II, 5 329-342, 1913.

[10] K. J. Laidler, Chemical Kinetics (Harper & Row Publishers, New York, 1987).

[11] J. M. Serra, PhD Thesis (University of Lisbon, 1995).

[12] Properties of Crystalline Silicon (R. Hull, INSPEC, 1999).

[13] J. Maia Alves et al, Review of Scientific Instruments 75 (2004) 5362-5363.

FIGURE CAPTIONS

Figure 1: Zone melting setup. Radiation from two halogen lamps is focused onto the sample surface creating a 2 mm wide molten zone. As the sample is moving downwards the molten zone travels upwards.

Figure 2: Fraction of boron oxide available on the surface of the silicon sample as a function of time. Model parameters: solution concentration 0.1365 mol/l, sample area 300 mm^2, initial boron oxide 9×10^{-8} kg.

Figure 3: Diffusion rate of atoms of boron into the sample. Model parameters: solution concentration 0.1365 mol/l, sample area 300 mm^2, initial boron oxide 9×10^{-8} kg.

Figure 4: Fraction of boron atoms diffused into the sample. Model parameters: solution concentration 0.1365 mol/l, sample area 300 mm^2, initial boron oxide 9×10^{-8} kg.

Figure 5: Photograph of silicon wafer with sprayed boric acid solution. Inset shows magnification of individual boric acid drop.

Figure 6: Mean boron incorporation as a function of boric acid initial concentration for typical run parameters.

Figure 7: Incorporation profiles for samples partially sprayed. The zero refers to edge of the sprayed area.

Figure 8: Boron incorporation rate for samples recrystallized with (1) molten zone moving upwards; (2) multipass molten zone, first upwards and then downwards; (3) molten zone moving downwards; and (4) multipass molten zone, first downwards and then upwards.

Figure 9: Variation of boron incorporation rate with argon flux. The vertical error bars represent the variations of incorporation along the samples.

FIG 1

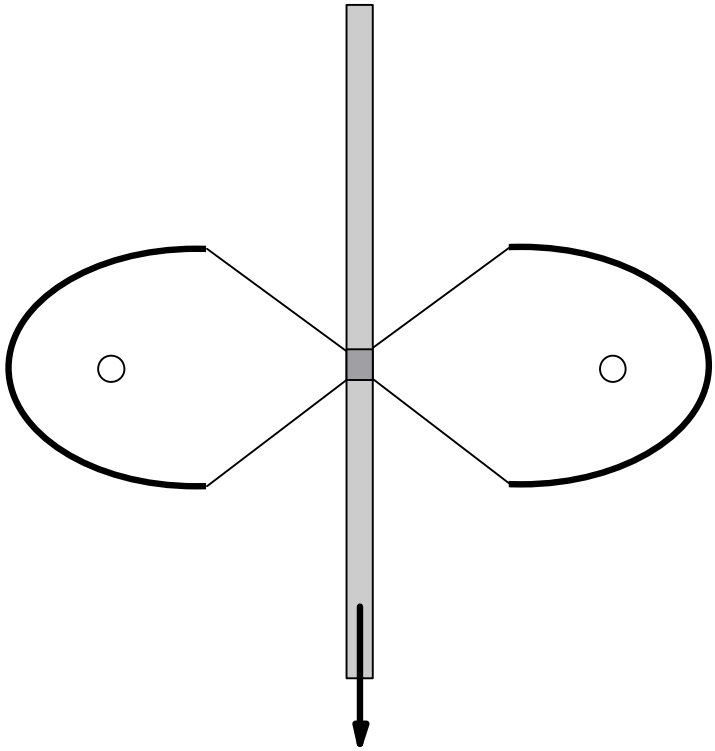

FIG 2

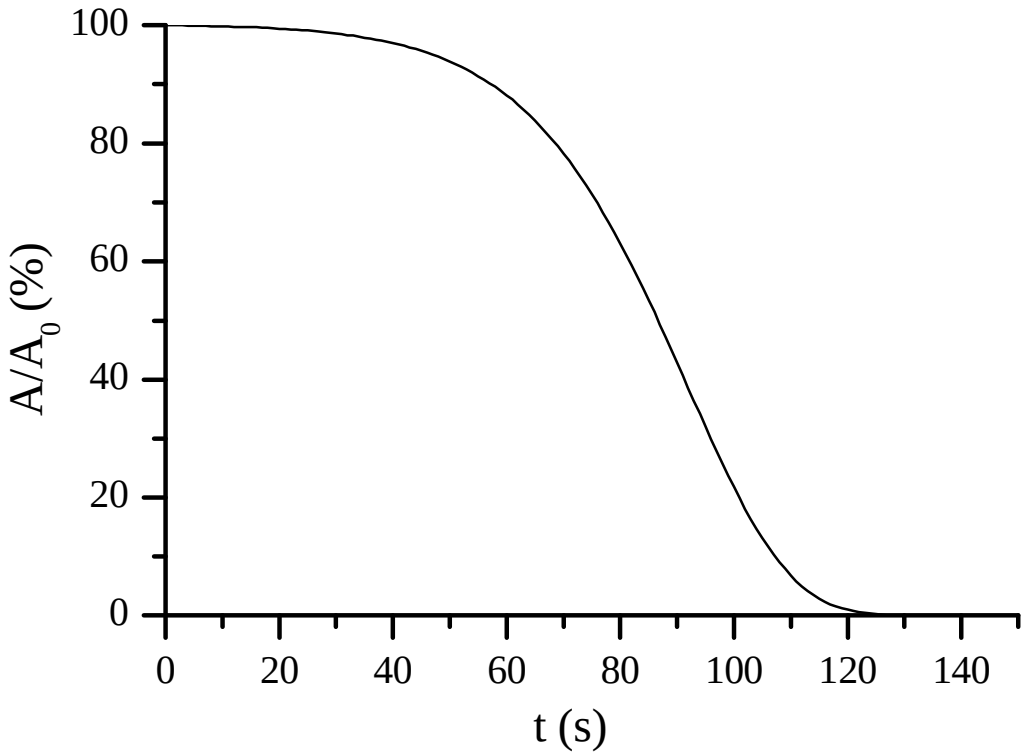

FIG 3

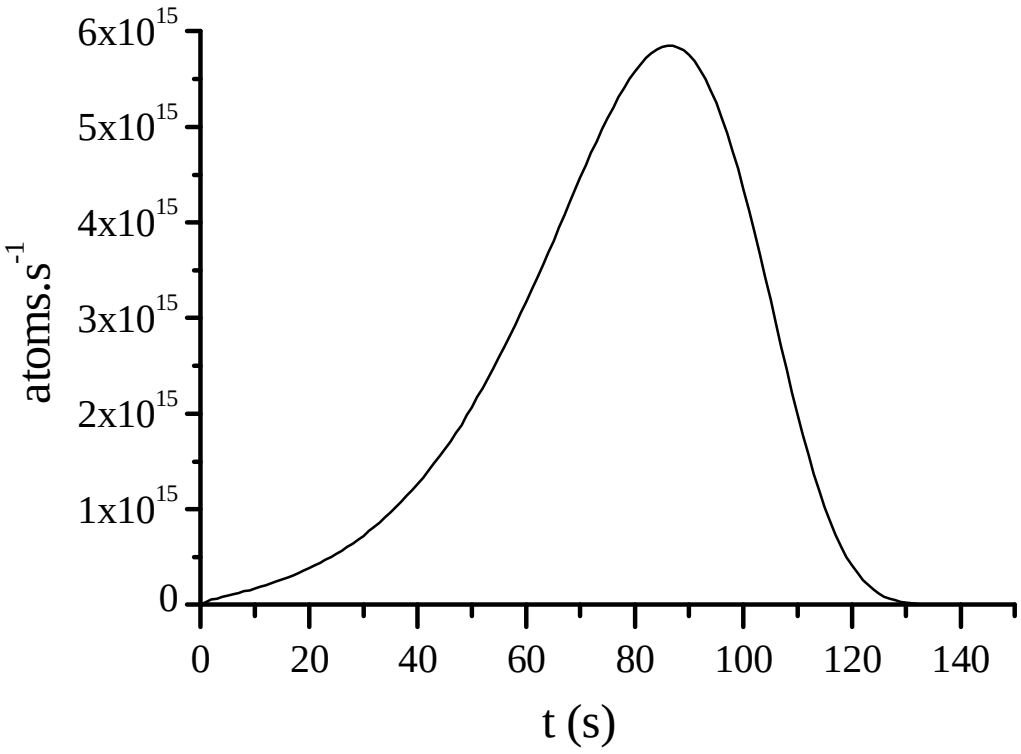
6x10^15
5x10^15
4x10^15
3x10^15
2x10^15
1x10^15
0
atoms.s^-1
0
20
40
60
80
100
120
140
t (s)

FIG 4

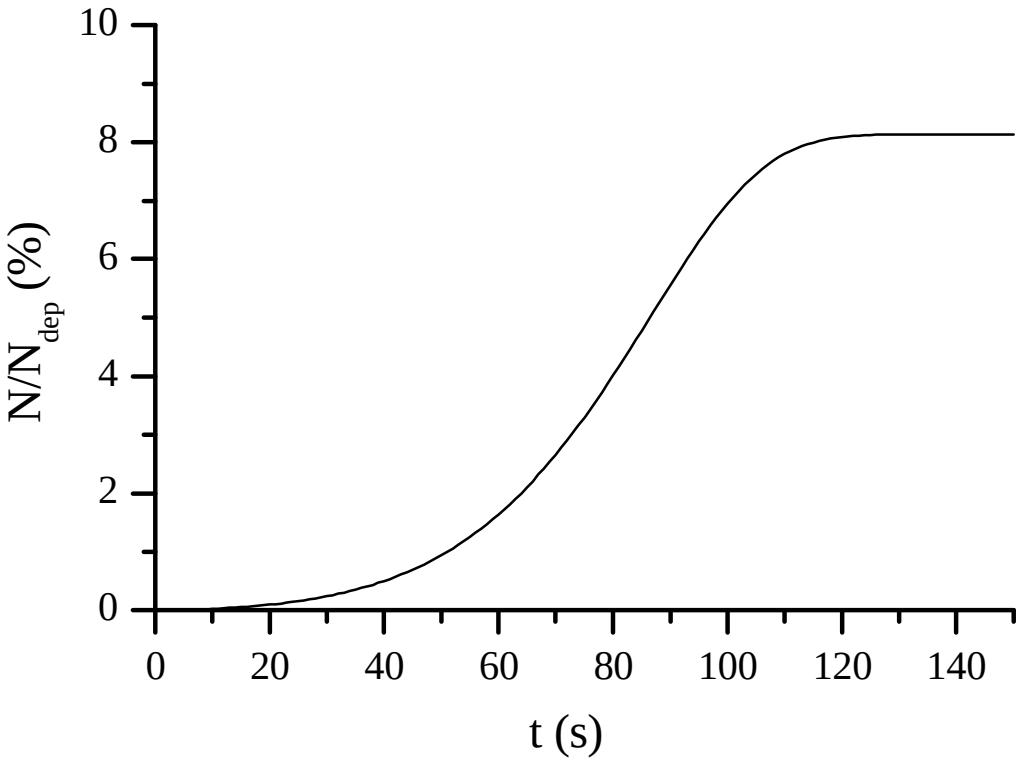

FIG 5

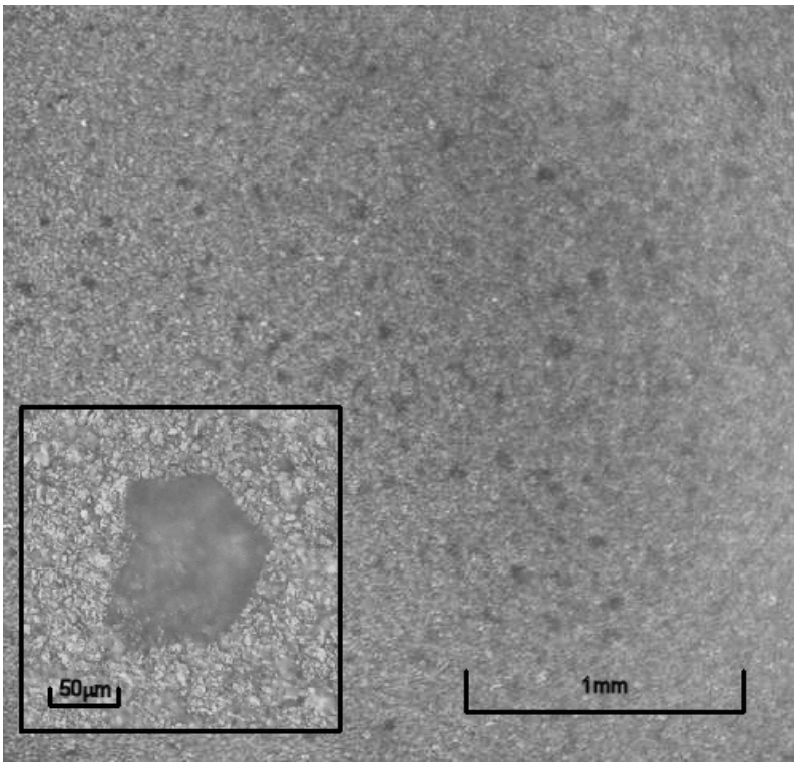

FIG 6

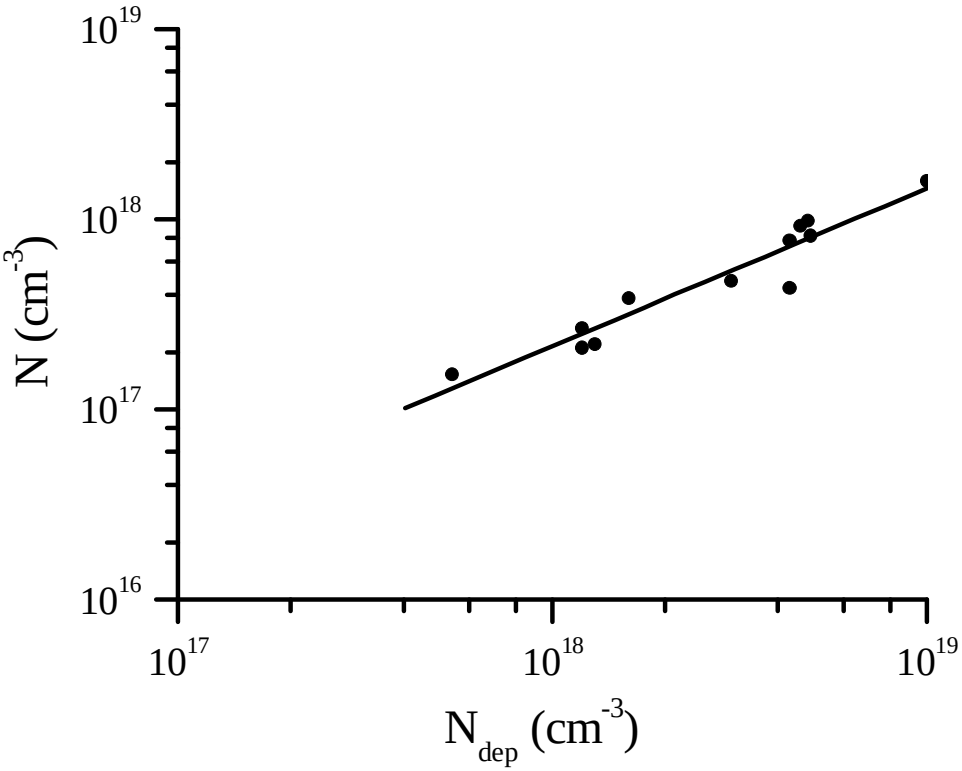

FIG 7

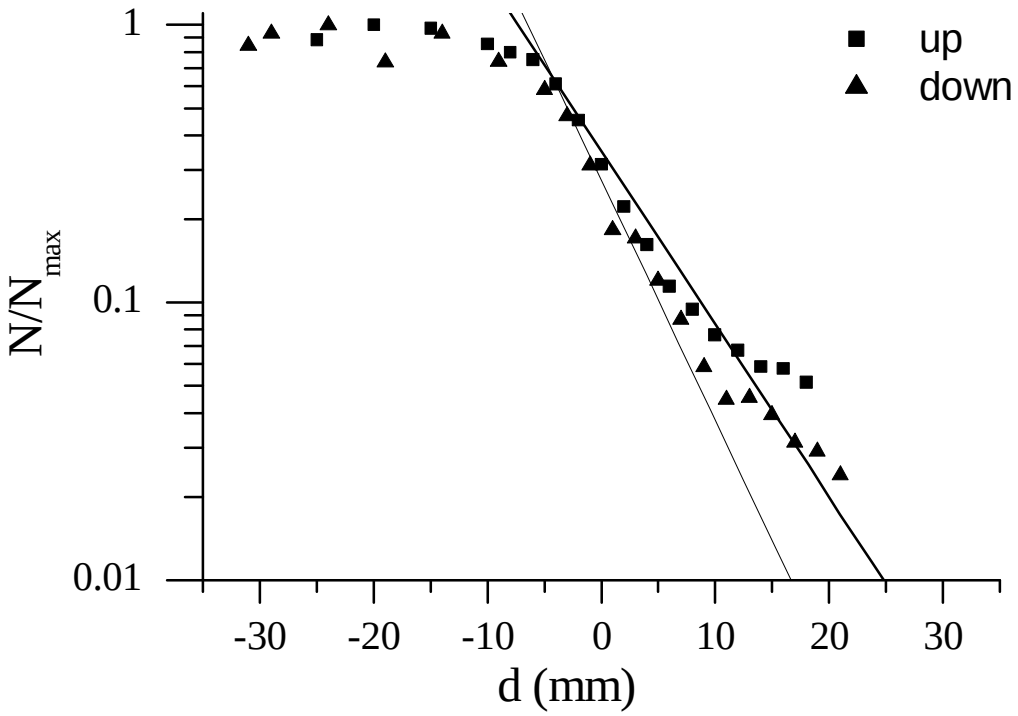

FIG 8

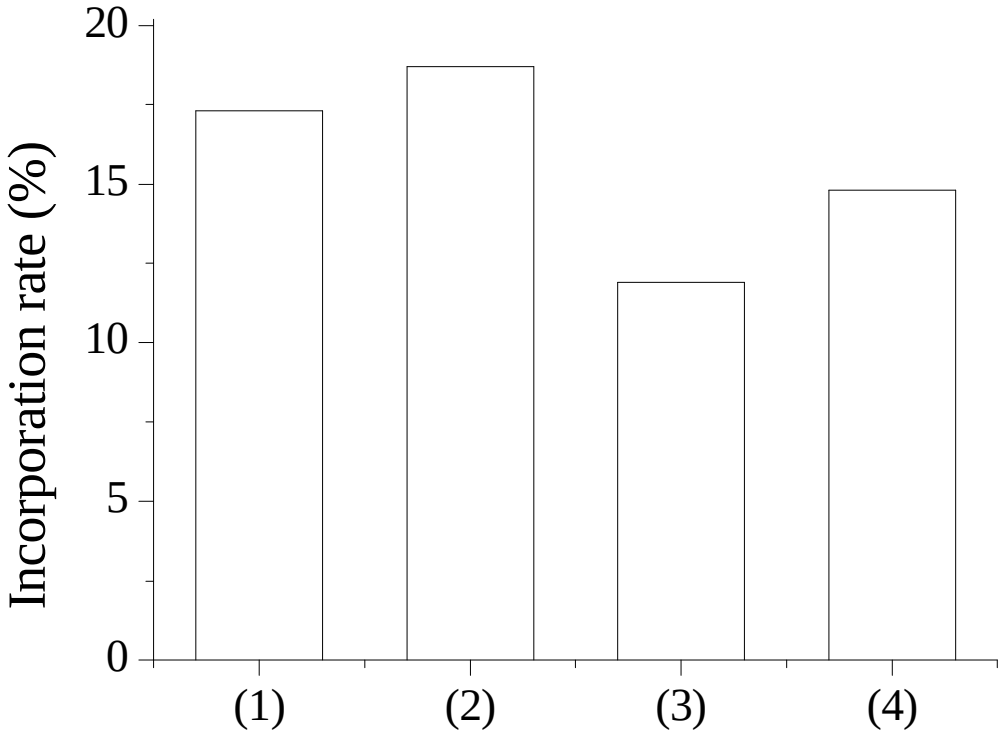

FIG 9